supplementary materials for

CTAB-induced synthesis of two-dimensional copper oxalate particles: Using L-ascorbic acid as the source of oxalate ligand

Bo Shen,[a] Zhengqiu Chen,[a] Huaming Mao,[b] Jungang Yin,[b] Yu Ren,[b] Wei Dai,[b] Shuanglong Zhao[b] and Hongwei Yang [*a, b]

[a] Kunming Institute of Precious Metals, Kunming, 650106, China.

[b] Yunnan Precious Metal Laboratory Co. Ltd., Kunming, 650106, China.

[*] Corresponding author.

Email: nanolab@ipm.com.cn.

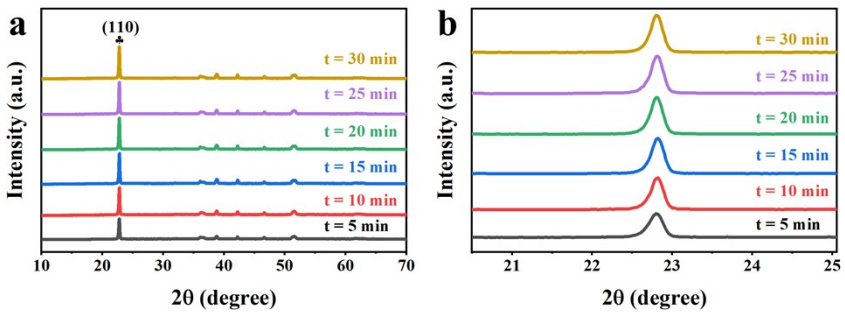

Fig. S1 XRD patterns of samples at 5 min intervals during synthesis (0-30 min) of copper oxalate (no CTAB added).

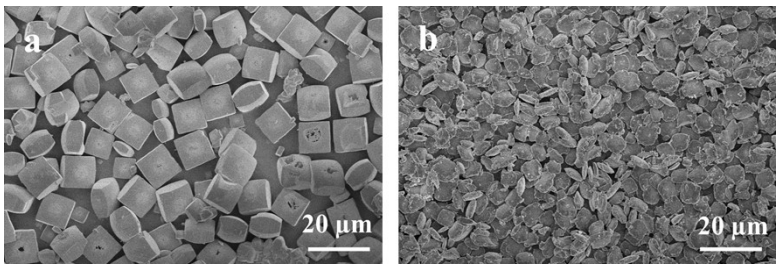

Fig. S2 SEM images of copper oxalate particles prepared in the magnification experiment. (a) No CTAB was added; (b) CTAB was added at 1 g/L.

Corresponding scale-up experiments were carried out, increasing the concentration of copper sulfate from around 20 mM to 400 mM. The corresponding experimental results showed that when CTAB was not added, the yield of square copper oxalate decreased slightly (from around 83% to 75%) and the particle size increased somewhat. When CTAB was added, the yield of copper oxalate (kept at about 85%) and the morphology were well preserved.

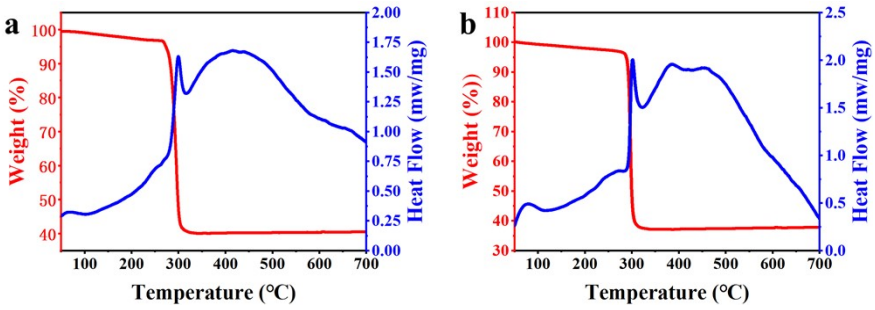

Fig. S3 TG-DSC curve of copper oxalate. (a) No CTAB was added; (b) CTAB was added at 1 g/L.

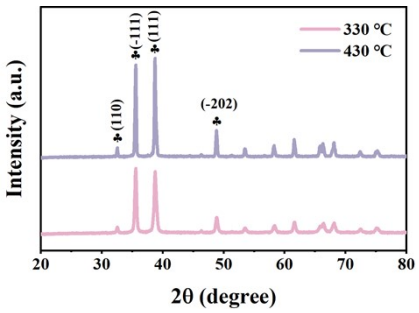

Fig. S4 XRD patterns of copper oxalate after calcination in air atmosphere.

After calcination of copper oxalate in air at 330 °C and 430 °C, respectively, the XRD results showed that the calcined products were all pure phase copper oxides. The major crystal planes and grain sizes of the products changed with the change of calcination temperature, which was further understood by SEM characterization.

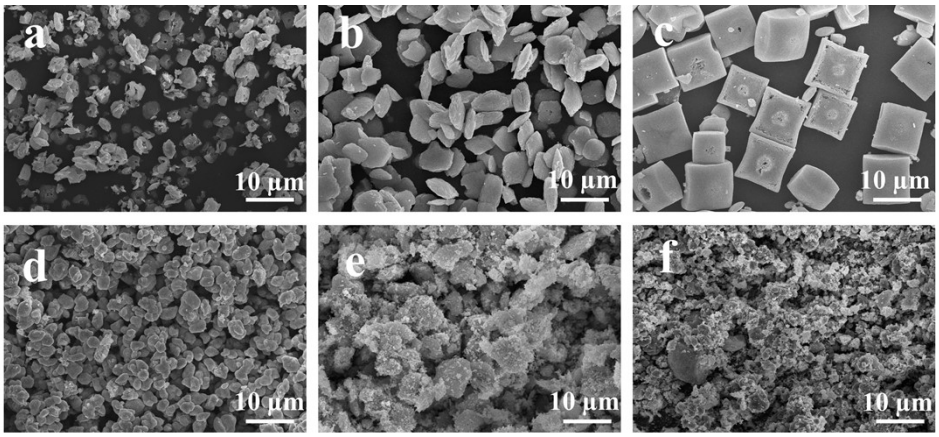

Fig. S5 SEM images of copper oxalate to after calcination in air atmosphere. SEM images after calcination at 330 °C: (a) CTAB addition of 0.1 g/L; (b) CTAB addition of 1 g/L; (c) no CTAB addition. SEM images after calcination at 430 °C: (d) CTAB addition of 0.1 g/L; (e) CTAB addition of 1 g/L; (f) no CTAB addition.

As shown in Fig. S5, the initial morphology and dispersion of the products were better preserved after calcination at 330 °C in air atmosphere, which is in agreement with the results of previous studies. However, in addition to this, the surface defects of the product shown in Fig. S5a were further aggravated, producing holes in the center of the raised surface of the product. This may originate from the release of residual H_2O_2 during the calcination process. The surface roughness of the product shown in Fig. S5b further increased, which may have led to the refinement of the product at higher temperatures. Surprisingly, the appearance of "nano box-like" product morphology in the products shown in Fig. S5c suggests that some unusual changes occurred in some of the products during the calcination process, which may be related to the fact that the preparation method used herein is different from the existing preparation methods.

After calcination at 430 °C in air atmosphere, all the products showed large agglomerates, which may be related to the increase in specific surface energy of the products after high-temperature refinement.

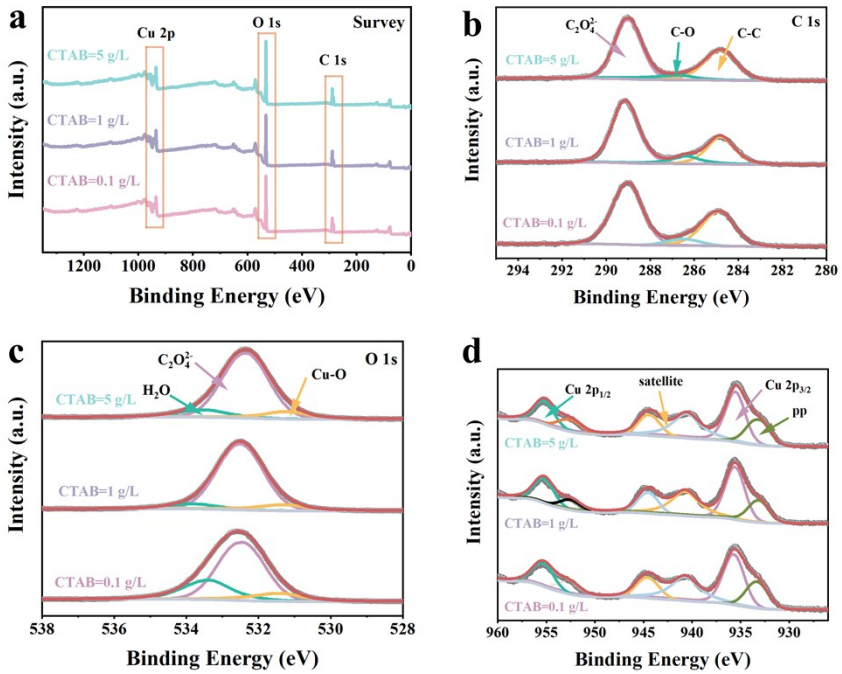

Fig. S6 XPS spectra of copper oxalate at different CTAB additions.

In agreement with the analysis in the XPS section of the manuscript, for all samples with different CTAB additions, only three elements, C, O and Cu, were detected on the sample surface, and no element N belonging to CTAB alone was detected, which again suggests that all CTAB with different additions were mostly removed during the washing process (Fig. S6a). The corresponding C 1s spectra all showed a typical bimodal structure (Fig. S6b). They can be separated into three peaks by deconvolution, which are attributed to non-fixed carbon C-C bonds, C-O bonds and $C_2O_4^{2-}$, respectively. The O 1s spectrum can be deconvoluted into three peaks corresponding to Cu-O bonds, $C_2O_4^{2-}$ and adsorbed water, respectively. In addition, the intensity of the peak attributed to adsorbed water decreases with increasing CTAB addition, which may be related to the exposure of long-chain alkyl groups with hydrophobicity in the CTAB molecular structure. In the high-resolution spectrum of Cu 2p, the intense satellite peaks located in the range of 938 eV-948 eV indicate that the valence state of elemental copper is +2. Moreover, an additional intensity peak (pp) was introduced to obtain a better fit in the low binding energy part of the spectrum. This

component (referred to as the "pre-peak") may be due to oxygen vacancies at neighboring sites formed during oxalate synthesis or vacancies generated by x-ray irradiation during XPS analysis.[17]

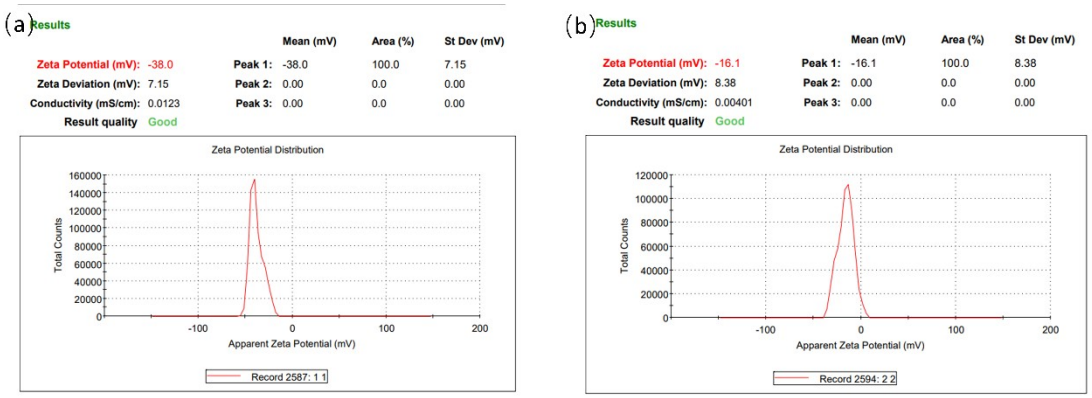

Fig. S7 Results of zeta potential testing of copper oxalate samples. (a) No CTAB was added; (b) CTAB was added and CTAB = 1 g/L.

S8. The method of HPLC test.

S8.1 Sample information

Sample preparation: Dissolve 0.6 g of L-ascorbic acid in 100 ml of deionized water to form a solution, stir in a water bath at 25 ℃ for 5 min, then add 1 ml of hydrogen peroxide solution with a mass concentration of 30%, and continue to keep stirring for 30 min to prepare the test sample.

Sample volume: about 5 ml for each sample;

S8.2 Equipment and materials

U3000 High Performance Liquid Chromatograph (Thermo Fisher Scientific); Acclaim Organic Acid LC liquid phase column (250 mm × 4 mm, 5 μm) was used.

Sodium sulfate (analytical pure), methanesulfonic acid (analytical pure), deionized water.

S8.3 Testing methods

S8.3.1 Sample treatment

The samples were processed at 80 ℃ for 5 h, then passed through 0.22 μm filter membrane and on the machine.

S8.3.2 Instrumental method/chromatographic conditions.

Chromatograph: Thermo Fisher U3000

Column temperature: 30 °C

Injection volume: 10 μL

Flow rate: 1 mL/min

UV detector: wavelength 214 nm

Mobile phase: 100 mM sodium sulfate, methanesulfonic acid adjusted to pH = 2.5.

Table S1 Synthesis of copper oxalate: a comparison of the methods in this manuscript with existing methods.

Method	Source of copper ion	oxalate ligand	Experimental conditions	Morphology	Ref.
Direct precipitation	$CuSO_4$	$H_2C_2O_4$	Vigorous stirring (1500 r/min) at room temperature; Incubated for 2 h.	orbicular	**1**
	$Cu(NO_3)_2$	$Na_2C_2O_4$	Boiling the stock solution twice to eliminate dissolved CO_2; Vigorous stirring (1500 r/min); Aging for 2 h.	cushion-like	**2**
	$CuCl_2$	$Na_2C_2O_4$	Vigorous stirring; Constant temperature.	disk-like	**3**
	$CuSO_4$	$H_2C_2O_4$	Adjust pH=2; Keep static for 48 h.	cushion-like; etched holes on the surface (PEG)	**4**
	$Cu(NO_3)_2$	$Na_2C_2O_4$	Requires masterbatch configuration; Adjust pH=5; Continuous mixing (500 r/min).	cushion-like; shift from cubes to bars (HPMC)	**5**
	$CuCl_2$	$(NH_4)_2C_2O_4$	Adjustment of pH by ammonia;	nanoflower	**6**
	$Cu(NO_3)_2$	$H_2C_2O_4$	Acetone as solvent.	orbicular	**7**
Microwave-assisted synthesis	$CuCl_2$	$H_2C_2O_4$	Stirring 1 h; 120 ℃ microwave heating 20 min.	orbicular	**8**
Solvothermal method	$Cu(CO_2CH_3)_2$	Diethyl oxalate	Heating at 100 ℃ for 12 h.	orbicular	**9**
Hydrothermal method	$CuCl_2$	$H_2C_2O_4$	Heating at 100 ℃ for 12 h.	nanopillars stacked into spheres	**10**
Precipitation-Stripping	$CuSO_4$	$H_2C_2O_4$	Extraction of copper with kerosene/LIX 84; Separation of the oil phase from the aqueous phase; Stripping of the copper-loaded oil phase in contact with oxalic acid and ethanol solutions.	Agglomerated spherical particles	**11, 12**
Ether–water bilayer refluxing system	$Cu(CO_2CH_3)_2$	Diethyl oxalate	Ether as solvent; 50 ℃ heating reflux 1 h.	nanowire	**13**
Ionic liquid-assisted synthesis	$Cu(CH_3COO)_2{\cdot}4H_2O$	$H_2C_2O_4$	$BMImBF_4$ as ionic liquid; Heating at 180 °C for 48 h.	nanowire	**14**
Hydrothermal method	$Cu(NO_3)_2$	L-ascorbic acid	Heating at 150 °C for 6 h.	orbicular	**15**
In situ precipitation	$CuSO_4$	L-ascorbic acid	H_2O_2 as oxidizing agent; Stirring at room temperature and pressure for 30 min.	Square-like shape without CTAB; shift to two-dimensional pie shape after addition of CTAB	this work

Table S2 Some comparisons of this manuscript with existing methods regarding similar copper oxalate morphology.

Ref.	Chemical Reagents	Additive	Condition	Drawback
[16]	$Na_2C_2O_4$ $CuSO_4$	EDTA	Simultaneous titration of precipitates; aging with stirring for different times	The low solubility of EDTA in water is not conducive to large-scale and high-yield synthesis of cake-like copper oxalate particles.
[3]	$Na_2C_2O_4$、$CuCl_2$	-	Oxalate ion solution as mother liquor; vigorous stirring.	Direct precipitation products tend to agglomerate; Vigorous stirring is a big safety hazard.
this work	$CuSO_4$、L-AA、H_2O_2	CTAB	Stirring at room temperature for 30 min.	The CTAB washing process is slightly more complicated.

References

[1] Z. Jia, L. Yue, Y. Zheng and Z. Xu, *Materials Research Bulletin*, 2008, **43**, 2434-2440.

[2] A. Aimable, A. Torres Puentes and P. Bowen, *Powder Technology*, 2011, **208**, 467-471.

[3] M. Rahimi-Nasrabadi, S. M. Pourmortazavi, A. A. Davoudi-Dehaghani, S. S. Hajimirsadeghi and M. M. Zahedi, *CrystEngComm*, 2013, **15**, 4077-4086.

[4] X. Zhao and J. Yu, *Journal of Crystal Growth*, 2007, **306**, 366-372.

[5] N. Jongen, P. Bowen, J. Lemaître, J.-C. Valmalette and H. Hofmann, *Journal of Colloid and Interface Science*, 2000, **226**, 189-198.

[6] Y.-q. Fan, C.-f. Zhang, J.-h. Wu, J. Zhan and P. Yang, *Transactions of Nonferrous Metals Society of China*, 2010, **20**, 165-170.

[7] G. Singh, I. P. S. Kapoor, R. Dubey and P. Srivastava, *Journal of Alloys and Compounds*, 2012, **513**, 499-505.

[8] Z. Qi, Y. Wu, X. Li, Y. Qu, Y. Yang and D. Mei, *Ionics*, 2019, **26**, 33-42.

[9] F. Behnoudnia and H. Dehghani, *Polyhedron*, 2013, **56**, 102-108.

[10] W. Kang and Q. Shen, *Journal of Power Sources*, 2013, **238**, 203-209.

[11] D. X. Zhang, H. Xu, Y. Z. Liao, H. S. Li and X. J. Yang, *Powder Technology*, 2009, **189**, 404-408.

[12] K. Shah, K. Gupta and B. Sengupta, *Powder Technology*, 2020, **366**, 230-238.

[13] N. Liang, W. Lei, S. Bing, W. Yinjue, Z. Wenli, W. Chao and J. Yong, *Materials Letters*, 2009, **63**, 2560-2563.

[14] M.-Y. Li, W.-S. Dong, C.-L. Liu, Z. Liu and F.-Q. Lin, *Journal of Crystal Growth*, 2008, **310**, 4628-4634.

[15] X.-L. Zhou, Z.-G. Yan and X.-D. Han, *Materials Letters*, 2014, **118**, 39-42.

[16] X. Chen, K. Huang and C.-y. Wang, *International Journal of Minerals, Metallurgy, and Materials*, 2018, **25**, 762-769.

[17] S. Chenakin and N. Kruse, *Applied Surface Science*, 2020, **515**, 146041.